



TITLE:

# Superconducting spin reorientation in spin-triplet multiple superconducting phases of UTe

AUTHOR(S):

Kinjo, Katsuki; Fujibayashi, Hiroki; Matsumura, Hiroki; Hori, Fumiya; Kitagawa, Shunsaku; Ishida, Kenji; Tokunaga, Yo; ... Li, Dexin; Honda, Fuminori; Aoki, Dai

---

CITATION:

Kinjo, Katsuki ...[et al]. Superconducting spin reorientation in spin-triplet multiple superconducting phases of UTe. *Science Advances* 2023, 9(30): eadg2736.

ISSUE DATE:

2023-07

URL:

<http://hdl.handle.net/2433/284529>

RIGHT:

Copyright © 2023 The Authors, some rights reserved; exclusive licensee American Association for the Advancement of Science. No claim to original U.S. Government Works. Distributed under a Creative Commons Attribution License 4.0 (CC BY); This is an open-access article distributed under the terms of the Creative Commons Attribution license, which permits unrestricted use, distribution, and reproduction in any medium, provided the original work is properly cited.



## PHYSICS

# Superconducting spin reorientation in spin-triplet multiple superconducting phases of $UTe_2$

Katsuki Kinjo<sup>1\*</sup>, Hiroki Fujibayashi<sup>1</sup>, Hiroki Matsumura<sup>1</sup>, Fumiya Hori<sup>1</sup>, Shunsaku Kitagawa<sup>1</sup>, Kenji Ishida<sup>1\*</sup>, Yo Tokunaga<sup>2</sup>, Hironori Sakai<sup>2</sup>, Shinsaku Kambe<sup>2</sup>, Ai Nakamura<sup>3</sup>, Yusei Shimizu<sup>3</sup>, Yoshiya Homma<sup>3</sup>, Dexin Li<sup>3</sup>, Fuminori Honda<sup>3,4</sup>, Dai Aoki<sup>3,5</sup>

Superconducting (SC) state has spin and orbital degrees of freedom, and spin-triplet superconductivity shows multiple SC phases because of the presence of these degrees of freedom. However, the observation of spin-direction rotation occurring inside the SC state (SC spin rotation) has hardly been reported. Uranium ditelluride, a recently found topological superconductor, exhibits various SC phases under pressure: SC state at ambient pressure (SC1), high-temperature SC state above 0.5 gigapascal (SC2), and low-temperature SC state above 0.5 gigapascal (SC3). We performed nuclear magnetic resonance (NMR) and ac susceptibility measurements on a single-crystal uranium ditelluride. The  $b$  axis spin susceptibility remains unchanged in SC2, unlike in SC1, and decreases below the SC2-SC3 transition with spin modulation. These unique properties in SC3 arise from the coexistence of two SC order parameters. Our NMR results confirm spin-triplet superconductivity with SC spin parallel to  $b$  axis in SC2 and unveil the remaining of spin degrees of freedom in SC uranium ditelluride.

## INTRODUCTION

What kind of an ordered state is realized under competing interaction is a central issue in condensed matter physics. Superconductivity and superfluidity are most remarkable macroscopic quantum phenomena produced by two fermion pairs, called the Cooper pair. In conventional superconductivity, which covers almost all superconductors found so far, the Cooper pairs have zero total spin and orbital angular momenta and have no degrees of freedom. Therefore, only one superconducting (SC) state is realized.

Theoretically, it is possible that either or both of the two angular momenta are nonzero, and hence, the coexistence of two SC phases, and/or multiple SC phases, was anticipated. The well-known example of such multiphases is the superfluid  $^3\text{He}$ , in which two phases (A and B) with the lowest energies are realized in zero field and becomes more complex under magnetic fields and/or anisotropic environment (1–4). The presence of the Majorana particles, which is applicable to “qubits” in quantum computer, was suggested in the surface state of the B phase (5). However, in superconductors, there are only limited examples for such multiple SC phases, for example,  $U\text{Pt}_3$  (6), Th-doped  $UBe_{13}$  (7), and  $\text{CeRh}_2\text{As}_2$  (8) are known so far. In addition, SC spin rotation, which is the smoking gun for the spin-triplet SC multiphase due to the presence of the spin degrees of freedom, has hardly been observed because of the tiny difference between the two critical temperatures (9). It is quite important to find textbook examples of the spin-triplet superconductivity, corresponding to the superfluid  $^3\text{He}$ ,

and to find the phenomena related to the spin and orbital degrees of freedom.

Here, we focus on a recently found uranium-based superconductor uranium ditelluride ( $UTe_2$ ) with SC transition temperature  $T_c \sim 1.6$  K (10).  $UTe_2$ , crystallizing orthorhombic structure with space group  $Immm$  (#71,  $D_{2h}$ ), as shown in Fig. 1A, has multiple SC phases. Under pressure ( $P$ ), the  $T_c$  of  $UTe_2$  increases to about 3 K at 1.2 GPa (11–13), as shown in Fig. 1B. Below 1.6 GPa, the two jumps in the temperature ( $T$ ) dependence of specific heat indicate the existence of at least two SC phases (11, 13): One exists at ambient pressure (SC1) and its  $T_c$  gradually decreases with applying  $P$ , and the other is an SC phase induced by  $P$  above 0.5 GPa (SC2), whose  $T_c$  has a maximum at 1.2 GPa. As a result,  $T_c$  of SC1 is below  $T_c$  of SC2 above 0.5 GPa, and thus, we call this SC state SC3 in this paper. Above 1.6 GPa, superconductivity suddenly disappears and a magnetic anomaly, which is considered as the antiferromagnetic state, was observed (13).

In addition,  $UTe_2$  shows multiple SC phases even at ambient pressure. For  $H||b$ ,  $T_c$  first decreases with increasing  $H$  and shows a minimum at around 16 T and then  $T_c$  increases up to 35 T (14). The bulk SC properties in the high-field SC (HFSC) phase were recently confirmed by thermodynamic and  $\chi_{ac}$  measurements (15, 16), suggesting that the pairing interaction grows up above 16 T (15).

Furthermore, recent nuclear magnetic resonance (NMR) measurements revealed a tiny change of spin susceptibility just below  $T_c$  for  $H||b$  and  $H||c$  (17–19), and almost no change in the  $a$  axis spin susceptibility (20). Above 14 T for  $H||b$ , spin susceptibility remains constant below  $T_c$  (16, 18). These results indicate that  $UTe_2$  is a spin-triplet superconductor with spin degrees of freedom and SC order parameter  $\mathbf{d}$  vector, which is perpendicular to the SC spin, having the  $b$  and  $c$  components in the low-field (LF) region. In  $UTe_2$ , a complex interplay of various interactions was reported, such as Ising-like ferromagnetic fluctuations from NMR studies (21) and the antiferromagnetic fluctuations from the inelastic neutron scattering measurements (22, 23). Such competing

<sup>1</sup>Department of Physics, Graduate School of Science, Kyoto University, Kyoto 606-8502, Japan. <sup>2</sup>Advanced Science Research Center, Japan Atomic Energy Agency, Tokai, Ibaraki 319-1195, Japan. <sup>3</sup>Institute for Materials Research, Tohoku University, Oarai, Ibaraki 311-1313, Japan. <sup>4</sup>Central Institute of Radioisotope Science and Safety, Kyushu University, Fukuoka 819-0395, Japan. <sup>5</sup>University Grenoble Alpes, CEA, Grenoble INP, IRIG, PHELIQS, F-38000 Grenoble, France.

\*Corresponding author. Email: katsuki.kinjo.c6@tohoku.ac.jp (K.K.); kishida@sphys.kyoto-u.ac.jp (K.I.)

†Present address: Institute of Multidisciplinary Research for Advanced Materials, Tohoku University, Sendai, Miyagi 980-8577, Japan.

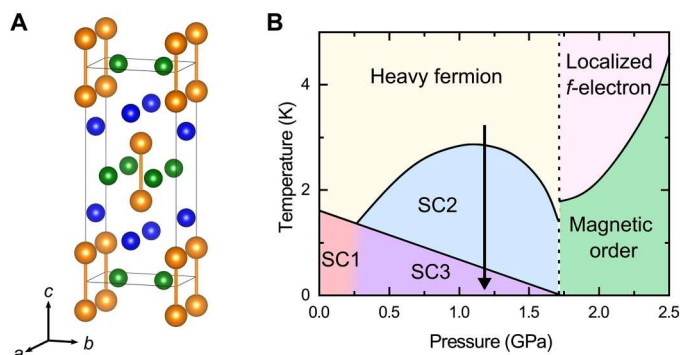


**Fig. 1. Crystal structure and pressure-temperature phase diagram of  $UTe_2$ .** (A) Crystal structure of  $UTe_2$  made by VESTA (39). The orange ball represents the U atom. The blue and green balls represent the Te(1) and Te(2) atom respectively. The U atom forms the dumbbell structure, and the dumbbells form a line along the  $a$  axis. (B) Pressure-temperature phase diagram of  $UTe_2$ . Bold lines correspond to the thermodynamic phase transitions detected by the specific heat measurements (11, 13). The phase boundary between SC1 and SC3 has not been detected. The arrow represents the measurement range in this report.

interactions are thought to induce rich physics such as the HFSC phase in  $H||b$  and multiple SC phases under pressure. Thus, identifying the SC properties of the SC2 and SC3 states is the last piece to understanding the multiple SC phases of  $UTe_2$ .

To elucidate the SC properties of the multiple SC phases in  $UTe_2$ , NMR serves as a highly effective tool. NMR is a technique that probes nuclear spins, which interact with electron spins through strong hyperfine interactions. Consequently, it enables us to investigate the electron spin susceptibility microscopically. While the spin susceptibility in the SC state cannot be measured because of SC diamagnetism by the bulk magnetization measurement, NMR can detect it with the hyperfine interaction. Moreover, to measure spin susceptibility in multiple SC states under pressure, NMR is a unique measurement that meets these requirements.

Here, we report the results of the NMR Knight shift  $K$  for  $H||b$  ( $K_b$ ) at 1.2 GPa, at which  $T_c$  of SC2 is maximum. We found that the spin susceptibility along the  $b$  axis is unchanged in SC2, which is different from that observed in SC1 at ambient pressure. More unexpectedly, at the SC2-SC3 transition,  $K_b$  suddenly decreases and the NMR spectral width becomes broader. These results suggest that the SC order parameter of SC1 and SC2 is different and that SC2 is a spin-triplet superconductivity with spin oriented toward the  $b$  axis and SC spin reoriented in SC3 state. These results suggest that the SC order parameter  $\mathbf{d}$  vector was changed at the SC3 transition, and the spin degrees of freedom remain in the superconductivity of  $UTe_2$ .

## RESULTS AND DISCUSSION

As there are two crystallographically inequivalent Te sites in  $UTe_2$ , we observed two  $^{125}\text{Te}$ -NMR peaks as reported in the previous paper (17–19): an NMR peak with the smaller (larger)  $K$  in  $H||b$  as Te(1) [Te(2)] by following the previous paper (21). The  $T$  variation of the NMR spectrum of Te(2) at  $P = 1.2$  GPa is shown in Fig. 2A, and the  $T$  dependence of the full width at half maximum (FWHM), the NMR Knight shift ( $K$ ) determined with the NMR spectrum, and  $\chi_{ac}$  are shown in Fig. 2B. Here, the NMR Knight

shift is proportional to the spin susceptibility, and the FWHM is proportional to the distribution of magnetization. As reported in the previous papers (24–26),  $K_b$  exhibits a broad maximum at  $T\chi_{\text{max}}$  and gradually decreases with decreasing  $T$ , similar to the  $T$  dependence of  $\chi$  (24). Owing to the increase in  $T_c$  and the decrease in  $T\chi_{\text{max}}$  with increasing  $P$  (24),  $K_b$  highly depends on  $T$  around  $T_c$  at 1.2 GPa, unlike the case of ambient pressure (0 GPa). To clarify the change in the Knight shift related to the SC transition, we calculate  $\Delta K \equiv K_{\text{SC}}^{\text{spin}} - K_{\text{normal}}^{\text{spin}}$  as shown in Fig. 3A. Here,  $K_{\text{normal}}^{\text{spin}}$  ( $K_{\text{SC}}^{\text{spin}}$ ) is  $K^{\text{spin}}$  in the normal (SC) state and is estimated from the extrapolation above  $T_c$ . Although the absolute value of the spin part in  $K$  ( $K_{\text{spin}}$ ) decreases with decreasing  $T$ ,  $\Delta K$  is almost zero above 0.5 K, indicating that the spin susceptibility in SC2 is the same as that in the normal state for  $H||b$ . This  $T$  dependence of the spin susceptibility in SC2 is similar to that in the A phase of the  $^3\text{He}$  superfluid (27). Below 0.5 K, we observed a sudden decrease in  $K_b$  and a broadening of the NMR spectrum, although no additional change was observed in  $\chi_{ac}$ . The magnitude of the decrease in  $K_b$  below 0.5 K is almost the same as that in  $K$  at 0 GPa (17). This is further evidence of the occurrence of the phase transition inside the SC state from the microscopic point of view.

Now, we consider possible SC order parameters suggested by the present NMR results. As discussed in the previous papers (17–20), the order parameter of spin-triplet superconductivity is  $\mathbf{d}$  vector, which is perpendicular to the SC spin components. In other words,  $K_i$  proportional to the spin susceptibility along the  $i$  axis decreases when  $\mathbf{d}$  vector has the  $i$  component, but is unchanged when the  $\mathbf{d}$  vector has no  $i$  component. This corresponds to the SC spin pointing to the  $i$  direction. The possible SC phases at zero field are listed in table 1 of (16). Our findings indicate that the  $\mathbf{d}$  vector has no  $b$  component (the SC spin is oriented to the  $b$  axis) in SC2 and has a finite  $b$  component in SC3, which is the same as that of SC1.

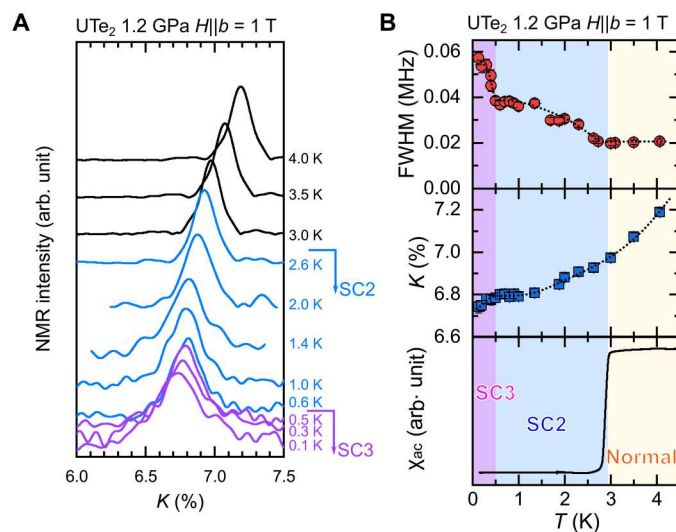


**Fig. 2. NMR evidence for SC spin rotation.** (A) Temperature variation of the NMR spectra of  $UTe_2$  at 1.2 GPa. (B) Temperature dependence of the FWHM, peak position  $K$  of Te(2) signal, and  $\chi_{ac}$  at 1.2 GPa. Line colors in (A) and background color in (B) represent the phase appearing in Fig. 1B. The kinks in the  $T$  dependence of  $K$  and FWHM suggest the phase transition at around 0.5 K, although  $\chi_{ac}$  does not show any anomaly. The dashed lines at the top and middle are guides to eye.

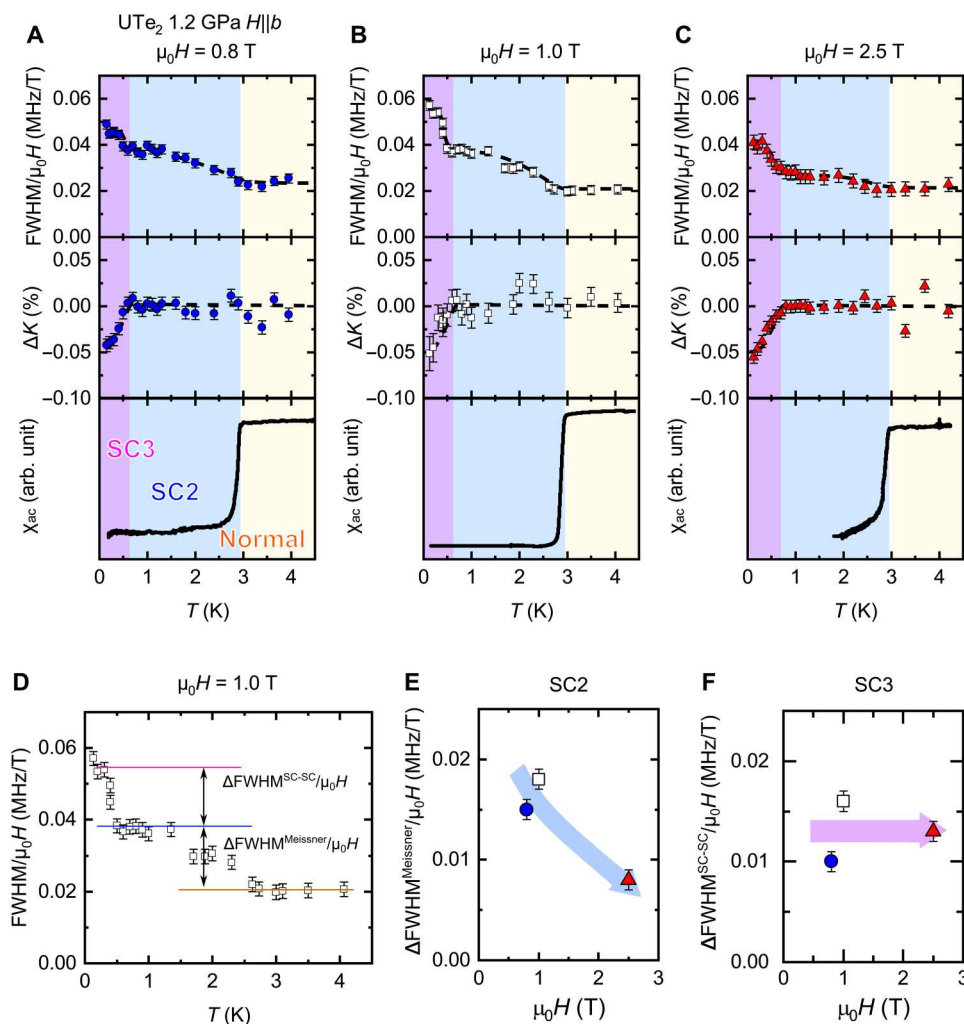


**Fig. 3. NMR data evidencing the increase in magnetic inhomogeneity.** Temperature dependence of (top) the  $FWHM/\mu_0 H$ , (middle)  $\Delta K$ , and (bottom)  $\chi_{ac}$  at (A) 0.8 T, (B) 1.0 T, and (C) 2.5 T of the Te(2) NMR spectrum. (D) The definition of  $\Delta FWHM^{Meissner}/\mu_0 H$  and  $\Delta FWHM^{SC-SC}/\mu_0 H$ , which are the NMR linewidth broadening in SC2 and SC3, respectively, is shown. The magnetic field dependence of (E)  $\Delta FWHM^{Meissner}/\mu_0 H$  and (F)  $\Delta FWHM^{SC-SC}/\mu_0 H$ . The definitions of these two are given in the main text.  $\Delta FWHM^{Meissner}/\mu_0 H$  decreases with applying field. This is conventional SC behavior and evidences the bulk superconductivity in the SC2 state.  $\Delta FWHM^{SC-SC}/\mu_0 H$  is almost constant against the field.

This is the  $\mathbf{d}$  vector rotation, evidencing the spin-triplet multiple SC phases with spin degrees of freedom.

Another important point of Fig. 2B is that the FWHM of the Te(2) site shows an additional increase below 0.5 K. Figure 3 (A to C) shows the temperature dependence of FWHM divided by the applied fields ( $\mu_0 H$ ), which reflects the distribution of the spin susceptibility,  $\Delta K$  measured at the Te(2) site, and  $\chi_{ac}$  measured at 0.8, 1.0, and 2.5 T, respectively. To clarify the increase in linewidth due to the normal-SC2 transition and the increase in linewidth due to the SC2-SC3 transition, we defined the values  $\Delta FWHM^{Meissner}$  and  $\Delta FWHM^{SC-SC}$ .  $\Delta FWHM^{Meissner}$  and  $\Delta FWHM^{SC-SC}$  are defined as  $FWHM(SC2) - FWHM(Normal)$  and  $FWHM(SC3) - FWHM(SC2)$ , respectively, as shown in Fig. 3D. In general, the FWHM of the NMR spectrum increases below  $T_c$  because of SC diamagnetism. This effect is related to the SC penetration depth, was observed below 3.0 K in SC2, and was suppressed with increasing  $\mu_0 H$ , as shown in Fig. 3E. Decrease of

$\Delta FWHM^{Meissner}/\mu_0 H$  with applying  $H$  is interpreted by the conventional SC diamagnetic effect. However, the additional increase in the FWHM below 0.5 K ( $\Delta FWHM^{SC-SC}/\mu_0 H$ ) cannot be explained by such SC diamagnetic effect, because  $\chi_{ac}$  shows no anomaly around 0.5 K, and  $\Delta FWHM^{SC-SC}/\mu_0 H$  is independent of the applied field, as shown in Fig. 3F. In addition, from the comparison of the NMR spectra between 0.6 K (SC2) and 0.13 K (SC3), it is noted that the spectrum shows a tail to the larger Knight shift side than the Knight shift in SC2 as shown in Fig. 4B. This is quite unusual for the NMR spectrum in the SC state, as the spin susceptibility decreases in the SC state. Such an NMR spectrum variation in the SC state was not observed in SC1 (Fig. 4A), although the spectrum broadening due to the SC diamagnetic effect was observed. The ratio between the FWHM of the Te(1) and Te(2) spectra in SC3 is almost unchanged to that in the normal state (28). These results indicate that the additional linewidth broadening in SC3 arises from the unusual inhomogeneity of the spin susceptibility,



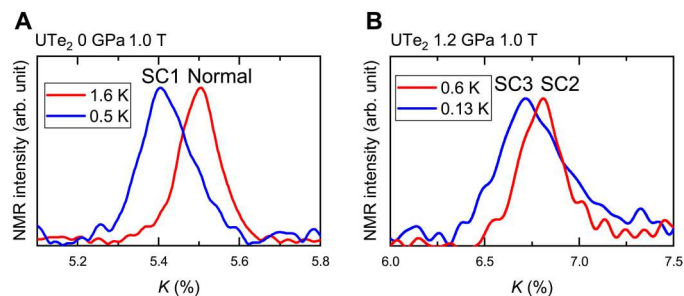


**Fig. 4. Comparison of the NMR spectrum broadening in SC1 and SC3.** (A) The NMR spectrum variation occurring in SC1. (B) The NMR spectrum broadening occurring in SC3. The spectrum in SC3 shows a tail to the larger Knight shift side than the Knight shift in SC2.

which was not observed in SC1. Thus, SC3 is a different SC state from SC1.

We consider the several possibilities of the origin of linewidth broadening in SC3. One is due to the SC vortex state in SC3. Because spin susceptibility is unchanged in SC2, the NMR signal from the vortex core is observed at almost the same position as the SC NMR signal outside the vortex. On the other hand, the spin susceptibility decreases in SC3, and the signal from the vortex core should be observed at the different position from the SC NMR signal, resulting in the NMR signal becoming broader in the mixed state of SC3. However, this possibility would be unlikely, because the measurement fields are far below  $H_{c2}^{orb} \sim 70$  T expected from the Werthamer, Helfand, and Hohenberg theory (29). Thus, the area fraction of the vortex is approximately 1%, and the contribution to the NMR spectrum is negligibly small. Another

possibility is spatial inhomogeneity with the coexistence of the two SC states in the sample. However, this possibility is ruled out, as the observed spectra could not be explained by the simple coexistence of the SC2 and SC3 states (28). These results indicate that, whatever the inhomogeneities in the sample, the NMR linewidth broadening intrinsically occurs below the SC2-SC3 transition and is proportional to the magnetic field. In other words, it represents an increase in the distribution of the magnetic susceptibility in the SC3 state. At present, we have no clear interpretation of this phenomenon, but we believe that we observed an effect because of the mixing of the two SC order parameters as in the case of (U,Th)Be<sub>13</sub> (30, 31). Actually, it was pointed out that the nonunitary spin-triplet superconductivity leads to a spin-density wave-type modulation of **d** vector from theoretical studies (32).

Figure 5 (A and B) shows the schematic image of  $T$  versus  $H$  along the  $b$  axis ( $H_b$ ) phase diagram of UTe<sub>2</sub> at ambient pressure (Fig. 5A) and 1.2 GPa (Fig. 5B) (13, 15, 18, 26). At ambient pressure,  $T_c(H)$  decreases in the LFSC (low-field SC) state and increases in the HFSC state up to the metamagnetic field 35 T ( $H_m$ ). In the LFSC state,  $K_b$  slightly decreases below  $T_c$  (see Fig. 5B) (17). As mentioned above,  $K_b$  is unchanged in the HFSC state (16), as shown in Fig. 5C, indicating that the SC spin aligns to the  $b$  axis. At the  $P \sim 1.2$  GPa where  $T_c$  becomes maximum,  $H_m$  is suppressed to almost half of  $H_m$  at  $P = 0$ , and there is no more L-shaped behavior in  $H_b$ - $T$  phase diagram (26). Considering the similarity in spin susceptibility in the SC state between the HFSC and SC2 states and first-order transition such as disappearance of SC state and Kondo coherent state with applying field or pressure (25, 33, 34), we conclude that the HFSC evolves into SC2 with applying pressure. In addition, the SC1 phase hides under the SC2 phase and becomes the

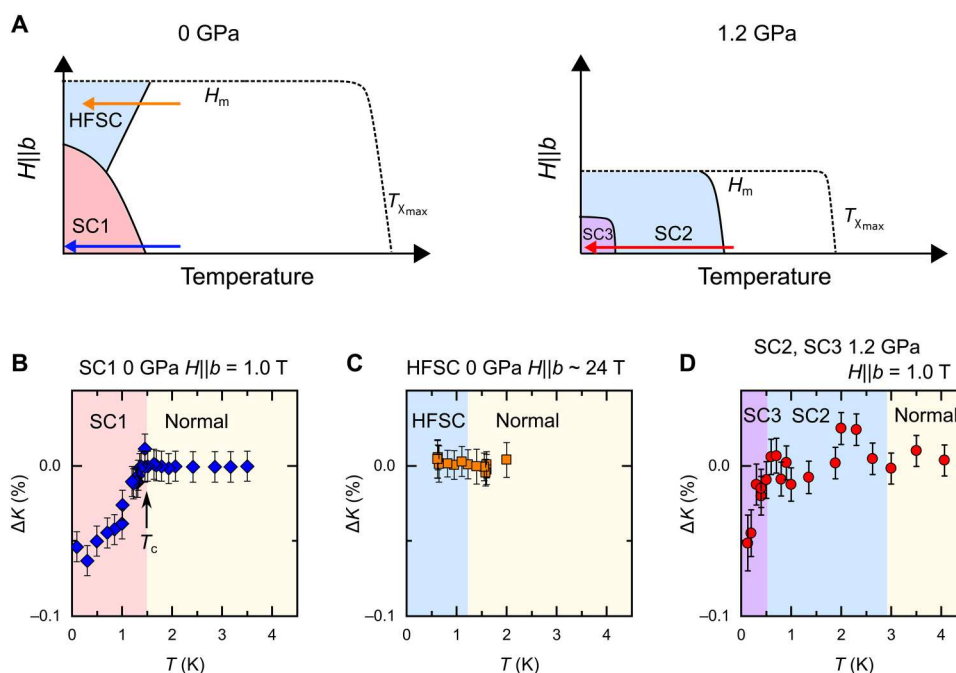


**Fig. 5. General phase diagram expected from our NMR results.** (A) The schematic images of the  $H$ - $T$  phase diagram of UTe<sub>2</sub> at 0 and 1.2 GPa. The bold lines are the transition lines determined by the thermodynamic measurements (11, 13, 15). The dashed line represents the temperature where the  $\chi_b$  shows maximum ( $T_{\chi_{max}}$ ) and metamagnetic transition. (B to D) The temperature dependence of  $\Delta K$  in four states appears in (A). The colored arrows in (A) represent the measurement range in (B) to (D).

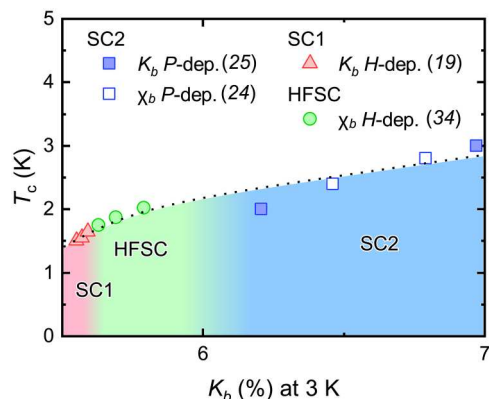


**Fig. 6. Relation between  $b$  axis susceptibility and critical temperature.** This diagram shows the relation between  $b$  axis magnetic susceptibility and the  $T_c$  of SC phases. For  $K_b$  between 5.7 and 6.0,  $T_c$  is affected by the magnetic field along the  $b$  axis. The extrapolation of  $T_c$  to  $H = 0$  in HFSC is based on the strong coupling parameter of Miyake *et al.* (34). The magnetic field enhances  $K_b$  and increases the  $T_c$ . As  $K_b$  increases further,  $T_c$  enters the SC2 region, and when  $K_b$  increases to nearly 7%,  $T_c$  increases to a maximum of 3 K. The dotted line is a guide to eyes.

SC3 phase (coexisting phase of SC1 and SC2), while the SC3 phase appears only inside the SC2 phase.

Another similarity between HFSC and SC2 is that  $T_c$  increases with increasing  $K_b$ ; Fig. 6 shows the values of  $K_b$  under magnetic field or under pressure. When a magnetic field is applied, the zero-field extrapolated  $T_c$  continues to increase with the application of the field (34), and  $K_b$  also increases. This tendency was also observed in the pressure experiment. When  $K_b$  is above 6.0%, indicating the sample in SC2,  $T_c$  increases up to 3 K with increasing  $K_b$ . The  $T_c$  versus  $K_b$  curves show similarity between under pressure and under magnetic field. It strongly suggests that HFSC and SC2 are similar phases and have the same origin. On the basis of this scenario, we suggest that the spin susceptibility along the  $b$  axis ( $\chi_b$ ) is an important parameter for HFSC and SC2, which determine the  $T_c$  of these states.

In conclusion, we have performed  $^{125}\text{Te}$ -NMR measurement on  $\text{UTe}_2$  under pressure to investigate the SC properties and determine the SC order parameter of SC2 and SC3 phases. The  $b$  axis spin susceptibility in SC2 has the same value as that of the normal state below 3.0 K above 0.5 K. Below 0.5 K, spin susceptibility decreases, and the NMR linewidth increases. These results indicate that the SC order parameter is changed, i.e., SC spin rotation occurs at the SC2-SC3 transition and the novel SC state with two SC order parameters in SC3. This is microscopic evidence for the remaining the spin degrees of freedom in the superconductivity of  $\text{UTe}_2$ , inherent to the spin-triplet superconductivity.

## MATERIALS AND METHODS

### Sample preparation

A high-quality single-crystal  $\text{UTe}_2$  sample was grown by the chemical vapor transport method, with iodine as a transport agent, details of which are described in (10, 35). The single crystal of  $\text{UTe}_2$  was an almost rectangular shape with 2 mm by 1 mm by 1 mm, with 2 mm along the  $a$  axis. To improve  $^{125}\text{Te}$ -NMR signal intensity, the sample was synthesized with the  $^{125}\text{Te}$ -enriched (99.9%) metal as discussed in (18). The  $T_c$  of this sample is 1.6 K at ambient pressure.

## ac susceptibility measurements

To confirm  $T_c$ , we measured the high-frequency ac susceptibility  $\chi_{ac}$  using the NMR tank circuit. In the SC state, the impedance of the circuit changes because of the Meissner effect, and thus, the tuning frequency of the circuit markedly changes just below  $T_c$ .

## Applying pressure and pressure estimation

The hydrostatic pressure is applied using a piston cylinder-type cell made of NiCrAl and CuBe alloys as described in (36). Daphne 7373 was used as a pressure medium. The applied pressure was estimated by the SC transition temperature of Pb with the formula of  $P = [7.181 - T_c(P)]/0.364$  (37).

## Field alignment

We used a split-pair magnet to apply horizontal fields to the sample and a  $^3\text{He}$ - $^4\text{He}$  dilution refrigerator that can be rotated about the vertical axis. With this setup, we could rotate the magnetic field direction within the  $bc$  plane of the sample. The direction of the magnetic field was confirmed by measuring the Te(1) signal as described in (24).

## NMR measurements

An NMR spectrometer with a 100 W (at 0 dB input) power amplifier (Thamway, product: N146-5049A) was used for the measurements. A conventional spin-echo method was used for NMR measurements in the temperature range from 0.1 to 4.2 K and in the magnetic field range from 0.8 to 2.5 T. All measurements were carried out with the  $^3\text{He}$ - $^4\text{He}$  dilution refrigerator, in which the pressure cell was immersed into the  $^3\text{He}$ - $^4\text{He}$  mixture to reduce radio frequency heating during measurements. The NMR spectrum was obtained by summation of the fast Fourier transform spectrum with a 5 kHz step. The applied field is estimated by  $^{65}\text{Cu}$ -NMR measurements as discussed here (38).

## Supplementary Materials

This PDF file includes:

- Supplementary Text
- Figs. S1 to S4
- References

## REFERENCES AND NOTES

- A. J. Leggett, A theoretical description of the new phases of liquid  $^3\text{He}$ . *Rev. Mod. Phys.* **47**, 331–414 (1975).
- J. C. Wheatly, Experimental properties of superfluid  $^3\text{He}$ . *Rev. Mod. Phys.* **47**, 415–470 (1975).
- H. Kojima, H. Ishimoto, Spin polarized superfluid  $^3\text{He}$  A<sub>1</sub>. *J. Phys. Soc. Jpn.* **77**, 111001 (2008).
- V. V. Dmitriev, M. S. Kutuzov, A. A. Soldatov, A. N. Yudin, Superfluid  $\beta$  phase of  $^3\text{He}$ . *Phys. Rev. Lett.* **127**, 265301 (2021).
- S. Murakawa, Y. Wada, Y. Tamura, M. Wasai, M. Saitoh, Y. Aoki, R. Nomura, Y. Okuda, Y. Nagato, M. Yamamoto, S. Higashitani, K. Nagai, Surface Majorana cone of the superfluid  $^3\text{He}$  B phase. *J. Phys. Soc. Jpn.* **80**, 013602 (2011).
- R. Joynt, L. Taillefer, The superconducting phases of  $\text{UPt}_3$ . *Rev. Mod. Phys.* **74**, 235–294 (2002).
- G. R. Stewart,  $\text{UBe}_{13}$  and  $\text{U}_{1-x}\text{Th}_x\text{Be}_{13}$ : Unconventional superconductors. *J. Low Temp. Phys.* **195**, 1–25 (2019).
- S. Khim, J. F. Landaeta, N. Bannor, M. Brando, P. M. R. Brydon, R. Cardoso-Gil, U. Stockert, A. P. Mackenzie, D. F. Agterberg, C. Geibel, E. Hassinger, Field-induced transition within the superconducting state of  $\text{CeRh}_2\text{As}_2$ . *Science* **373**, 1012–1016 (2021).

9. H. Tou, Y. Kitaoka, K. Ishida, K. Asayama, N. Kimura, Y. Onuki, E. Yamamoto, Y. Haga, K. Maezawa, Nonunitary spin-triplet superconductivity in UPt<sub>3</sub>: Evidence from <sup>195</sup>Pt Knight shift study. *Phys. Rev. Lett.* **80**, 3129–3132 (1998).
10. S. Ran, C. Eckberg, Q.-P. Ding, Y. Furukawa, T. Metz, S. R. Saha, I.-L. Liu, M. Zic, H. Kim, J. Paglione, N. P. Butch, Nearly ferromagnetic spin-triplet superconductivity. *Science* **365**, 684–687 (2019).
11. D. Braithwaite, M. Vališka, G. Knebel, G. Lapertot, J.-P. Brison, A. Pourret, M. E. Zhitomirsky, J. Flouquet, F. Honda, D. Aoki, Multiple superconducting phases in a nearly ferromagnetic system. *Commun. Phys.* **2**, 147 (2019).
12. S. Ran, H. Kim, I.-L. Liu, S. R. Saha, I. Hayes, T. Metz, Y. S. Eo, J. Paglione, N. P. Butch, Enhancement and reentrance of spin triplet superconductivity in UTe<sub>2</sub> under pressure. *Phys. Rev. B* **101**, 140503 (2020).
13. S. M. Thomas, F. B. Santos, M. H. Christensen, T. Asaba, F. Ronning, J. D. Thompson, E. D. Bauer, R. M. Fernandes, G. Fabbris, P. F. S. Rosa, Evidence for a pressure-induced antiferromagnetic quantum critical point in intermediate-valence UTe<sub>2</sub>. *Sci. Adv.* **6**, eabc8709 (2020).
14. G. Knebel, W. Knafo, A. Pourret, Q. Niu, M. Vališka, D. Braithwaite, G. Lapertot, J.-P. Brison, S. Mishra, I. Sheikin, G. Seyfarth, D. Aoki, J. Flouquet, Field-reentrant superconductivity close to a metamagnetic transition in the heavy-fermion superconductor UTe<sub>2</sub>. *J. Phys. Soc. Jpn.* **88**, 063707 (2019).
15. A. Rosuel, C. Marcenat, G. Knebel, T. Klein, A. Pourret, N. Marquardt, Q. Niu, S. Rousseau, A. Demuer, G. Seyfarth, G. Lapertot, D. Aoki, D. Braithwaite, J. Flouquet, J. P. Brison, Field-induced tuning of the pairing state in a superconductor. *Phys. Rev. X* **13**, 011022 (2023).
16. K. Kinjo, H. Fujibayashi, S. Kitagawa, K. Ishida, Y. Tokunaga, H. Sakai, S. Kambe, A. Nakamura, Y. Shimizu, Y. Homma, D. X. Li, F. Honda, D. Aoki, K. Hiraki, M. Kimata, T. Sasaki, Change of superconducting character in UTe<sub>2</sub> induced by magnetic field. *Phys. Rev. B* **107**, L060502 (2023).
17. G. Nakamine, S. Kitagawa, K. Ishida, Y. Tokunaga, H. Sakai, S. Kambe, A. Nakamura, Y. Shimizu, Y. Homma, D. X. Li, F. Honda, D. Aoki, Superconducting properties of heavy fermion UTe<sub>2</sub> revealed by <sup>125</sup>Te-nuclear magnetic resonance. *J. Phys. Soc. Jpn.* **88**, 113703 (2019).
18. G. Nakamine, K. Kinjo, S. Kitagawa, K. Ishida, Y. Tokunaga, H. Sakai, S. Kambe, A. Nakamura, Y. Shimizu, Y. Homma, D. Li, F. Honda, D. Aoki, Anisotropic response of spin susceptibility in the superconducting state of UTe<sub>2</sub> probed with <sup>125</sup>Te-NMR measurement. *Phys. Rev. B* **103**, L100503 (2021).
19. G. Nakamine, K. Kinjo, S. Kitagawa, K. Ishida, Y. Tokunaga, H. Sakai, S. Kambe, A. Nakamura, Y. Shimizu, Y. Homma, D. Li, F. Honda, D. Aoki, Inhomogeneous superconducting state probed by <sup>125</sup>Te NMR on UTe<sub>2</sub>. *J. Phys. Soc. Jpn.* **90**, 064709 (2021).
20. H. Fujibayashi, G. Nakamine, K. Kinjo, S. Kitagawa, K. Ishida, Y. Tokunaga, H. Sakai, S. Kambe, A. Nakamura, Y. Shimizu, Y. Homma, D. Li, F. Honda, D. Aoki, Superconducting order parameter in UTe<sub>2</sub> determined by Knight shift measurement. *J. Phys. Soc. Jpn.* **91**, 043705 (2022).
21. Y. Tokunaga, H. Sakai, S. Kambe, T. Hattori, N. Higa, G. Nakamine, S. Kitagawa, K. Ishida, A. Nakamura, Y. Shimizu, Y. Homma, D. Li, F. Honda, D. Aoki, <sup>125</sup>Te-NMR study on a single crystal of heavy fermion superconductor UTe<sub>2</sub>. *J. Phys. Soc. Jpn.* **88**, 073701 (2019).
22. C. Duan, K. Sasmal, M. B. Maple, A. Podlesnyak, J.-X. Zhu, Q. Si, P. Dai, Incommensurate spin fluctuations in the spin-triplet superconductor Candidate UTe<sub>2</sub>. *Phys. Rev. Lett.* **125**, 237003 (2020).
23. W. Knafo, G. Knebel, P. Steffens, K. Kaneko, A. Rosuel, J.-P. Brison, J. Flouquet, D. Aoki, G. Lapertot, S. Raymond, Low-dimensional antiferromagnetic fluctuations in the heavy-fermion paramagnetic ladder compound UTe<sub>2</sub>. *Phys. Rev. B* **104**, L100409 (2021).
24. D. Li, A. Nakamura, F. Honda, Y. J. Sato, Y. Homma, Y. Shimizu, J. Ishizuka, Y. Yanase, G. Knebel, J. Flouquet, D. Aoki, Magnetic properties under pressure in novel spin-triplet superconductor UTe<sub>2</sub>. *J. Phys. Soc. Jpn.* **90**, 073703 (2021).
25. K. Kinjo, H. Fujibayashi, G. Nakamine, S. Kitagawa, K. Ishida, Y. Tokunaga, H. Sakai, S. Kambe, A. Nakamura, Y. Shimizu, Y. Homma, D. Li, F. Honda, D. Aoki, Drastic change in magnetic anisotropy of UTe<sub>2</sub> under pressure revealed by <sup>125</sup>Te-NMR. *Phys. Rev. B* **105**, L140502 (2022).
26. G. Knebel, M. Kimata, M. Vališka, F. Honda, D. Li, D. Braithwaite, G. Lapertot, W. Knafo, A. Pourret, Y. J. Sato, Y. Shimizu, T. Kihara, J.-P. Brison, J. Flouquet, D. Aoki, Anisotropy of the upper critical field in the heavy-fermion superconductor UTe<sub>2</sub> under pressure. *J. Phys. Soc. Jpn.* **89**, 053707 (2020).
27. R. F. Hoyt, H. N. Scholz, D. O. Edwards, Superfluid <sup>3</sup>He-B: The dependence of the susceptibility and energy gap on magnetic field. *Physica B+C* **107**, 287–288 (1981).
28. Supporting information are available as Supplementary Materials.
29. N. R. Werthamer, E. Helfand, P. C. Hohenberg, Temperature and purity dependence of the superconducting critical field, H<sub>c2</sub>. III. Electron spin and spin-orbit effects. *Phys. Rev.* **147**, 295 (1966).
30. R. H. Heffner, J. L. Smith, J. O. Willis, P. Birrer, C. Baines, F. N. Gygax, B. Hitti, E. Lippelt, H. R. Ott, A. Schenck, E. A. Knetsch, J. A. Mydosh, D. E. MaLaughlin, New phase diagram for (U,Th)Be<sub>13</sub>: A muon-spin-resonance and H<sub>c1</sub> study. *Phys. Rev. Lett.* **65**, 2816 (1990).
31. S. K. Ghosh, M. Smidman, T. Shang, J. F. Annett, A. D. Hiller, J. Quintanilla, H. Yuan, Recent progress on superconductors with time-reversal symmetry breaking. *J. Phys. Condens. Matter* **33**, 033001 (2021).
32. M. Sigrist, T. M. Rice, Phenomenological theory of the superconductivity phase diagram of U1-xThx. *Phys. Rev. B Condens Matter* **39**, 2200–2216 (1989).
33. S. Imajo, Y. Kohama, A. Miyake, C. Dong, M. Tokunaga, J. Flouquet, K. Kindo, D. Aoki, Thermodynamic investigation of metamagnetism in pulsed high magnetic fields on heavy fermion superconductor UTe<sub>2</sub>. *J. Phys. Soc. Jpn.* **88**, 083705 (2019).
34. A. Miyake, Y. Shimizu, Y. J. Sato, D. Li, A. Nakamura, Y. Homma, F. Honda, J. Flouquet, M. Tokunaga, D. Aoki, Metamagnetic transition in heavy fermion superconductor UTe<sub>2</sub>. *J. Phys. Soc. Jpn.* **88**, 063706 (2019).
35. D. Aoki, A. Nakamura, F. Honda, D. Li, Y. Homma, Y. Shimizu, Y. J. Sato, G. Knebel, J.-P. Brison, A. Pourret, D. Braithwaite, G. Lapertot, Q. Niu, M. Vališka, H. Harima, J. Flouquet, Unconventional superconductivity in heavy fermion UTe<sub>2</sub>. *J. Phys. Soc. Jpn.* **88**, 043702 (2019).
36. N. Fujiwara, N. Mōri, Y. Uwatoko, T. Matsumoto, N. Motoyama, S. Uchida, Superconductivity of the Sr<sub>2</sub>Ca<sub>12</sub>Cu<sub>24</sub>O<sub>41</sub> spin-ladder system: Are the superconducting pairing and the spin-gap formation of the same origin? *Phys. Rev. Lett.* **90**, 137001 (2003).
37. B. Bireckoven, J. Witting, A diamond anvil cell for the investigation of superconductivity under pressures of up to 50 GPa: Pb as a low temperature manometer. *J. Phys. E Sci. Instrum.* **21**, 841–848 (1988).
38. K. Kitagawa, H. Gotou, T. Yagi, A. Yamada, T. Matsumoto, Y. Uwatoko, M. Takigawa, Space efficient opposed-anvil high-pressure cell and its application to optical and NMR measurements up to 9 GPa. *J. Phys. Soc. Jpn.* **79**, 024001 (2010).
39. K. Momma, F. Izumi, VESTA 3 for three-dimensional visualization of crystal, volumetric and morphology data. *J. Appl. Crystallogr.* **44**, 1272–1276 (2011).
40. A. Pustogov, Y. Luo, A. Chronister, Y.-S. Su, D. A. Sokolov, F. Jerzembeck, A. P. Mackenzie, C. W. Hicks, N. Kikugawa, S. Raghu, E. D. Bauer, S. E. Brown, Constraints on the superconducting order parameter in Sr<sub>2</sub>RuO<sub>4</sub> from oxygen-17 nuclear magnetic resonance. *Nature* **574**, 72–75 (2019).
41. K. Ishida, M. Manago, K. Kinjo, Y. Maeno, Reduction of the <sup>17</sup>O Knight shift in the superconducting state and the heat-up effect by NMR pulses on Sr<sub>2</sub>RuO<sub>4</sub>. *J. Phys. Soc. Jpn.* **89**, 034712 (2020).
42. K. Kinjo, M. Manago, S. Kitagawa, Z. Q. Mao, S. Yonezawa, Y. Maeno, K. Ishida, Superconducting spin smecticity evidencing the Fulde-Ferrell-Larkin-Ovchinnikov state in Sr<sub>2</sub>RuO<sub>4</sub>. *Science* **376**, 397–400 (2022).

**Acknowledgments:** We thank A. Miyake, Y. Yanase, Y. Matsuda, K. Machida, S. Fujimoto, V. P. Mineev, Y. Maeno, S. Yonezawa, J.-P. Brison, G. Knebel, and W. Knafo for valuable discussions. **Funding:** This work was supported by the Kyoto University LTM Center. This work was supported by Grants-in-Aid for Scientific Research (grant nos. JP19K03726, JP19K14657, JP19K21840, JP19H04696, JP19H00646, JP20H00130, JP20KK0061, JP21K18600, JP22H04933, JP22H01168, JP22K03516, and JP23H01124). This work was also supported by JST SPRING (grant number JPMJSP2110). K.K., H.F., and H.M. would like to acknowledge the support from the Motizuki Fund of Yukawa Memorial Foundation. **Author contributions:** K.I., Y.T., and D.A. implemented this project. A.N., Y.S., Y.H., D.L., F.Hon., and D.A. synthesized and characterized the samples. K.K., H.F., H.M., F.Hor., S.Ki., K.I., Y.T., H.S., and S.Ka. performed the NMR measurements and analysis. K.K., H.F., H.M., F.Hor., S.Ki., and K.I. drafted the manuscript. **Competing interests:** The authors declare that they have no competing interests. **Data and materials availability:** All data needed to evaluate the conclusions in the paper are present in the paper and/or the Supplementary Materials, or on Zenodo at DOI: 10.5281/zenodo.8051080.

Submitted 13 December 2022  
Accepted 23 June 2023  
Published 28 July 2023  
10.1126/sciadv.adg2736

# ScienceAdvances

## Superconducting spin reorientation in spin-triplet multiple superconducting phases of $UTe_2$

Katsuki Kinjo, Hiroki Fujibayashi, Hiroki Matsumura, Fumiya Hori, Shunsaku Kitagawa, Kenji Ishida, Yo Tokunaga, Hironori Sakai, Shinsaku Kambe, Ai Nakamura, Yusei Shimizu, Yoshiya Homma, Dexin Li, Fuminori Honda, and Dai Aoki

*Sci. Adv.*, **9** (30), eadg2736.  
DOI: 10.1126/sciadv.adg2736

### View the article online

<https://www.science.org/doi/10.1126/sciadv.adg2736>

### Permissions

<https://www.science.org/help/reprints-and-permissions>

Use of this article is subject to the [Terms of service](#)

---

*Science Advances* (ISSN ) is published by the American Association for the Advancement of Science. 1200 New York Avenue NW, Washington, DC 20005. The title *Science Advances* is a registered trademark of AAAS.  
Copyright © 2023 The Authors, some rights reserved; exclusive licensee American Association for the Advancement of Science. No claim to original U.S. Government Works. Distributed under a Creative Commons Attribution License 4.0 (CC BY).